Journal of New Technology and Materials (JNTM)
J. New Technol. Mater.
Vol. 08, N°02 (2018)16-23

OEB Univ. Publish. Co.

Study of AlGaN/GaN MOS-HEMTs with TiO_2 gate dielectric and regrown source/drain

Z. Touati [a*], Z. Hamaizia[a] and Z. Messai[b, c]

[a]*Laboratory of Semiconducting and Metallic Materials, University of Mohamed KhiderBiskra, Algeria.*
[b]*Electronics Department, Faculty of Sciences and Technology, University of BBA, Algeria*
[c]*Laboratory of Optoelectronics and Components, UFAS 19000, Algeria*
*Corresponding author, email: zinouu113@yahoo.fr

Received date: Oct. 15, 2017; revised date: June 03, 2018; accepted date: Sep. 18, 2018

Abstract

In this work, we proposed a novel TiO_2/AlGaN/GaN metal-oxide-semiconductor high electron mobility transistor model (MOS-HEMT) with 60 nm gate-length and high-k TiO_2 gate dielectric. The DC and RF characteristics of the proposed AlGaN/GaN MOS-HEMT structure were obtained using the TCAD Silvaco Software. It showsa maximum extrinsic transconductance of 198.3 mS/mm, a saturated drain-current density at V_{GS} = 4 V of 668.4 mA/mm, with a maximum of 677.9 mA/mm, a unity-gain cut-off frequency of 229.8 GHz, and an impressive maximum oscillation frequency of 627.8 GHz. Characterized at 10 GHz, the power performance of the proposed device showsan output power of 22.3 dBm, a power gain of 13.1 dB, and a power-added efficiency of 26.5%.The obtained simulated results are very encouraging while compared to existing AlGaN/GaN MOS-HEMTs. This is, in fact, the best TiO2/AlGaN/GaN MOS-HEMT simulated high-frequency performance reported so far, making it suitable for high-power RF circuit applications.

Keywords: TiO_2/AlGaN/GaN; MOS-HEMT; high-k, TiO_2; Regrown Source/Drain; SILVACO.

1. Introduction

GaN-based High Electron Mobility Transistors (HEMTs) are quite suitable devices for high-power and high-frequency applications, due to their appropriate material properties such as high breakdown voltage, high saturation velocity, low effective mass, high thermal conductivity and high two-dimensional electron gas (2DEG) density, in the order of 10^{13} cm^{-2},produced by spontaneous and piezoelectric polarization in AlGaN/GaN hetero-structures[1-3].However, Schottky gate transistors usually exhibit high gate leakage current [4], making the drain current to collapse when operating at high frequencies [5]thus, limiting the performance and reliability of HEMTs in RadioFrequency (RF) power applications.

Metal Oxide Semiconductor HEMTs (MOS-HEMTs) with insulating dielectric have beenwidely investigated, andexcellent performance have been reported using various high-k insulators(Al_2O_3[4-6], TiO_2[7-9], HfO_2[10, 11], Pr_2O_3[12, 13],SiN[14], SiO_2[14] and NiO [15]).

in [16], Hong-Yu et al. asserted that SiO_2-gate AlGaN/GaN HEMTs show good electrical performance such as high unity-gain cut-off frequency f_t and maximum oscillation frequency f_{max}, low gate leakage, small threshold voltage V_{TH} fluctuation and small current collapse. However, high leakage currents were observed in MOS-HEMTs underforward biasconditions[17-19], probably due toinsufficient AlGaN bandgaps [16]. In addition, Deen et al. [17]and Hayashi et al. [20]reported severeV_{TH}fluctuations from HEMTs with HfO_2-gate dielectric materials while Stoklas et al. [21]described similar instability issues in HEMTs with ZrO_2-gate dielectric materials. Therefore, further investigation is necessary to gain better understanding of high-kinsulators/(Al)GaN interfaces.

Furthermore, all these devices suffer from a high contact resistance (of about 0.3Ω·mm) and high on-resistance (of about 1Ω·mm) due to the alloyed ohmic contacts and large source-drain distance. Recently, n+ regrown source/drain regions have become a novel approach leading to non-alloyed ohmic contacts and a self-aligned gate process[22, 23].

In this work, the DC and microwave characteristics of a novel AlGaN/GaN MOS-HEMT with 5-nm-thick TiO_2 dielectric layer,60 nm gate-length,and 10nm heavily doped (n++ InGaN) regrown ohmic source/drain regions was investigated.

Using the commercial TCAD Silvaco Software, the proposed TiO2/AlGaN/GaN MOS-HEMT deviceexhibitsa maximum extrinsic transconductance (g_m) of 198.3 mS/mm, a saturated I_{DS} density of 668.4 mA/mm at V_{GS} = 4 V, with a maximum at 677.9 mA/mm, a unity-gain cut-off frequency (f_t) of 229.8 GHz, as well as an impressive maximum oscillation frequency f_{max} of 627.8 GHz. In terms of power performance, it can deliver an output power (P_{out}) of 22.3

dBm, a power gain of 13.1 dB, and a power-added efficiency (PAE) of 26.5%at 10 GHz, making it suitable for high-power RF circuit applications.

2. Device description and simulation models

2.1. The oxide choice

As reported in Table.1,among variousgate dielectric materials[24], TiO_2can beconsidered as the most suitable candidate because of its large static dielectric constant (k= 86–170). Previous research works[25-27]showed that transistors, with TiO_2 as gate dielectric,demonstratea high breakdown voltage and very low gate leakage current, along with a slight decrease in g_m and small shift in V_{TH}.

Table 1: High-k dielectric materials and their properties[24].

Gate dielectric Material	Dielectric constant (k)	Energy bandgap Eg (eV)	Conduction band offset ΔEc (eV)	Valence band offset ΔEc(eV)
SiO_2	3.9	9	3.5	4.4
Al_2O_3	8	8.8	3	4.7
TiO_2	80	3.5	1.1	1.3
ZrO_2	25	5.8	1.4	3.3
HfO_2	25	5.8	1.4	3.3

2.2. The device structure

Figure.1 shows the cross-sectional schematic of the proposed $TiO_2/Al_{0.3}GaN_{0.7}$/GaN MOS-HEMT device with source/drain regrowth. The gate length and width are of 60 nm and 20 nm respectively, thesource/drain length is of 0.5µm, while both source-gate and gate drain spacing are of 0.33 µm. The oxide thickness is 5 nm with TiO_2 dielectric to minimize leakages.AGaN buffer layer of 0.8 µm thickness (doped with [donor] = 2.5×10^{18} cm^{-3})wasadopted and grown on top of the SiC semi-insulating substrate.

An AlN nucleation layer has been inserted to reduce stress and lattice mismatch, with an undoped GaN channel thickness of 20 nm. A 7 nm $Al_{0.3}GaN_{0.7}$ barrier layer, which depletes the 2DEG,provides a strong carrier confinementin the quantum well at the hetero-interface and minimizes the junction leakage and the off-state leakage current I_{off}.

Next, a graded n+ $In_{0.3}Ga_{0.7}N$ (10 nm), doped with [donor] = 2×10^{19} cm^{-3}, wasintroducedto reduce the access and contact resistances[22].Non-alloyed contacts wereformed for the source/drain regions to give a low contact resistance. Apassivation of the SiO_2layer over the dielectric surface wasused to reduce thesurface trap density tofurther improve the device characteristics.

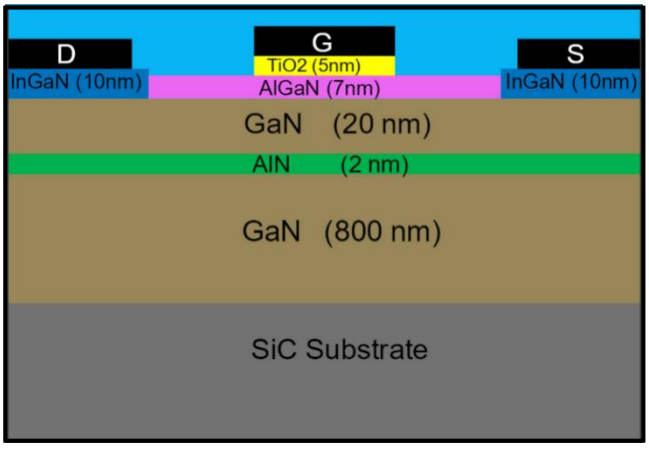

Figure 1.Cross-section structure of the proposed $TiO_2/Al_{0.3}GaN_{0.7}$/GaN MOS-HEMT.

2.3. Physical models

Simulations wereperformed using the Two-Dimensional (2D) Silvaco ATLAS TCAD tool. The Boltzmann transport theory has shown that the current densities in the continuity equations may be approximated by a drift-diffusion model (DD).This model is one of the most basic carrier transport model in semiconductorphysics. In this case, the current densities for electrons and holes under the DD model can be expressed as

$$\vec{J}_n = -nq\mu_n \nabla \emptyset_n \quad (1)$$

$$\vec{J}_n = -nq\mu_p \nabla \emptyset_p \quad (2)$$

where n and p state for the respective electron and hole concentrations, and μ_n and $\mu_p$for therespective electron and hole mobilities. Φ_n and $\Phi_p$represent the respective electron and hole quasi-fermi potentials.

Based on the DD model, the Poisson equation (3), the electron continuity equation (4) and the hole continuity equation (5), were numerically solved[28]. A drift-diffusion model wasused to solve the transport equation.

$$div(\varepsilon \nabla \Psi) = -\rho \quad (3)$$

$$\frac{dn}{dx} = \frac{1}{q}\nabla \vec{J}_n + G_n - R_n \quad (4)$$

$$\frac{dp}{dx} = \frac{1}{q}\nabla \overrightarrow{J_n} + G_p - R_p \quad (5)$$

withεthe permittivity,Ψ the electrostatic potential, q the electron charge, and ρ the space charge density.($\vec{J}$n,Gn,Rn)

and ($\vec{J}$p, Gp, Rp)state for the current densities, generation rates, and recombination rates for respectively the electrons and holes.

The consideredphysical models in the simulations include Shockley-Read Hall recombination (SRH), Fermi-Dirac statistics, Multiband k.p., GaNFET model and field-dependent mobility [29].

3. Results

3.1. Energy band diagram of MOS-HEMT

Figure.2 shows the energy band of the $TiO_2/Al_{0.3}GaN_{0.7}/GaN$ MOS-HEMT biased at V_{GS} = 1 V and V_{DS} = 0.5 V. When V_{GS} is sweptfrom -10 V to 1 V, the captured electrons begin to be thermally emitted into the AlGaN conduction band. The blue arrows show a possible path of the thermally emittedelectrons from the capture states: (1) electrons emitted from trap states to the conduction band of the AlGaN layer, at the TiO_2 /AlGaN interface; (2) electrons at the AlGaN conduction band 'rolling down' to the triangular quantum well at the AlGaN/GaN interface due to the potential difference across the thickness of the AlGaN layer. This causes the 2DEG to appear at the AlGaN/GaN interface; (3) electrons are swept away laterally due to V_{DS}.

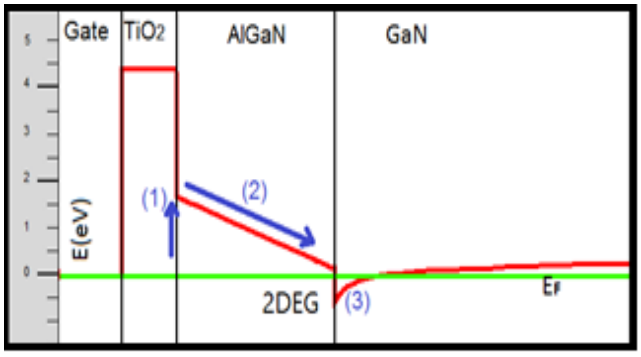

Figure 2. Energy band of the $TiO_2/Al_{0.3}GaN_{0.7}/GaN$ MOS-HEMT under the gate electrode.

3.2. DC results

DC simulations were performed in Silvacoby sweeping the gate voltage from -10 V to 10 V and the drain voltage from 0 V to 6 V. The I_{DS}-V_{DS} curves of Figure.3 allowed evaluatingsomeMOS-HEMT parameterssuch as the knee voltage (transition between the triodeand saturation regions), the on-resistance, as well as the maximum current and self-heating. The device exhibited a peak current density of 638 mA/mm at V_{GS} = 2 V and 687 mA/mm at V_{GS}=10 V. However, the device didnot pinch off completely even at a gate bias of -6V. As documented by Breitschadel etal [30], Zhongda et al [31]and Park etal[32], this is probably due to the short-channel effect, since the simulated device has a gate length of 60 nm.

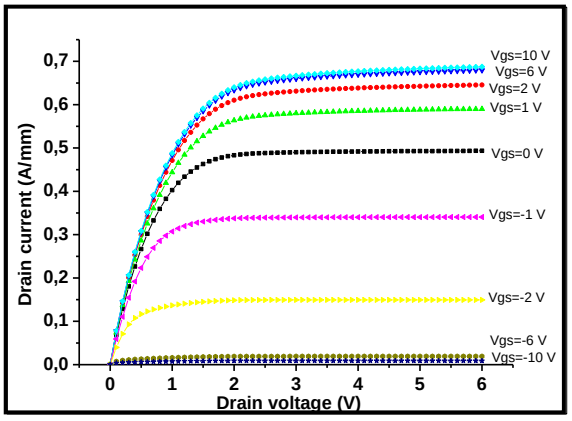

Figure 3. I_{DS}-V_{DS}DC characteristics of the simulated $TiO_2/Al_{0.3}GaN_{0.7}$ GaN MOS- HEMT.

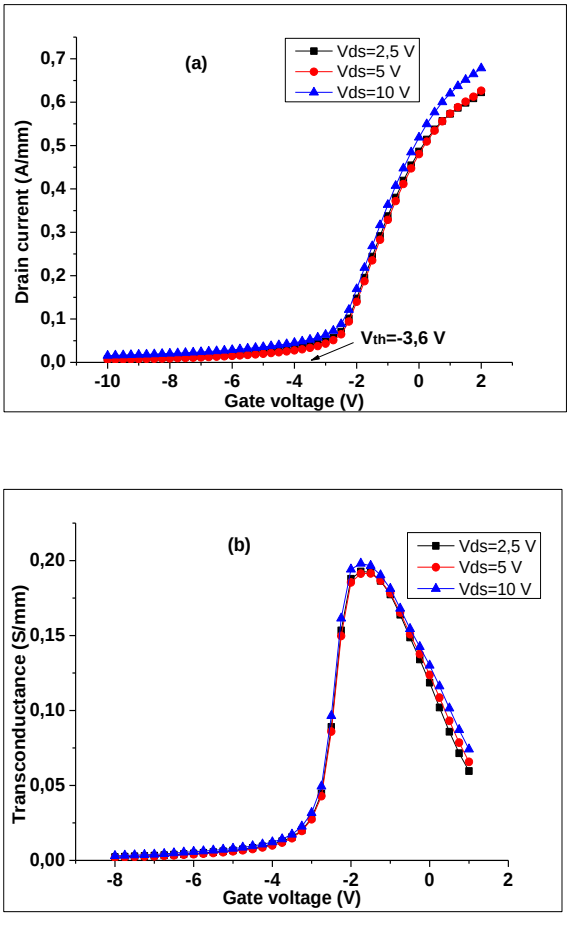

Figure 4. (a)Transfercharacteristic, (b) transconductance at V_{DS} =2.5 V,5 V and 10 V.

As shown in Figure 4 (a), the threshold voltage V_{TH} is about -3.6 V. The transconductance g_m (Figure.4 (b)) was obtained by deriving the I_{DS}-V_{GS} curves at fixed V_{DS}, showing a peak of about 200 mS/mm.

3.3. Analysis of traps and defects

Traps can be caused by defects in the material, that can be related to crystal defects, polluting agents and mismatch between different layers[33]. The trapping process results also in strong dependenciesof the I-V characteristics in drain-source voltage slowdynamics [34].

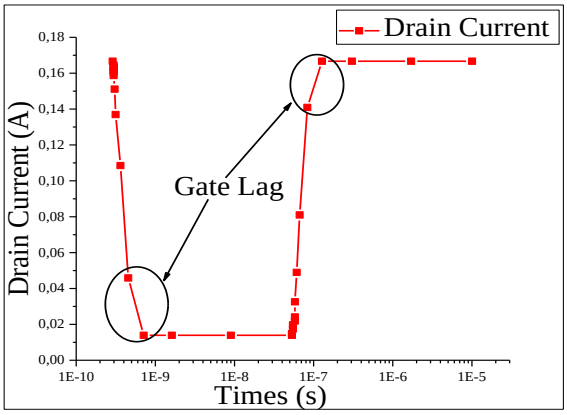

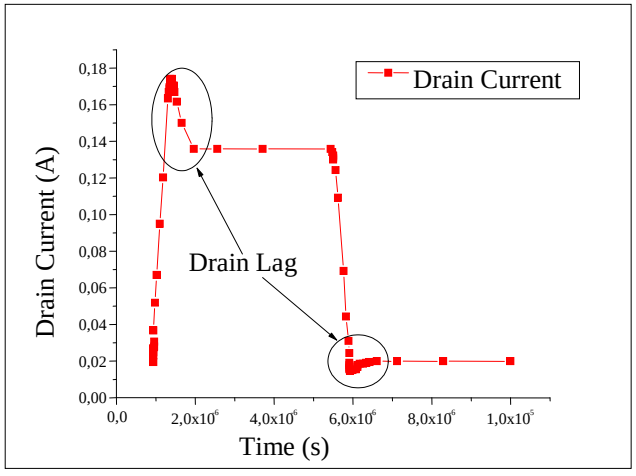

Figure 5. (a) Gate Lag and (b) Drain Lag of the TiO_2/AlGaN/GaN MOS-HEMT.

From an electrical point of view, when characterizing TiO_2/$Al_{0.3}GaN_{0.7}$/GaN MOS-HEMT, the traps can beseparated into two types "Gate Lag" and "Drain Lag" [34], corresponding to the delayed response of the drain current associated with the V_{GS} and V_{DS} control voltages, respectively. Note thatdrain-lag effects can be considered as self-back gatingeffectscaused by deep traps under the channel.

Since each effect depends only on its respective drain or gate voltage, in frequency domain, the impact of gate-lag is noticeable on the transconductance (the partial derivative of the drain current with respect to V_{GS}) while the impact of drain-lag is focused on the output conductance (the partial derivative of the drain current with respect to V_{DS}) [35]. Analysis of the drain- and gate-lag effects is a good indicator of the device RF performance. A device with reduced gate- and drain-lag can be accurately predicted to showimproved RF performance, withhigherf$_t$ and f$_{max}$. According to the simulation results shownin Figure.5, it is clearthat the GaN MOS-HEMT examined in this work showed both gate- and drain-lag.

The calculated gate-lag and drain-lag percentages are given in Table.2. Since our device displays an acceptabledrain-lag of 13.6 % and gate-lag of 5.3 %, we can then conclude that our device reaches its steady state promptly.

Table 2:Calculated gate-lag and drain-lag percentage.

Gate-lag (%)	Drain-lag (%)
5.3	13.6

3.4. Impact ionization:

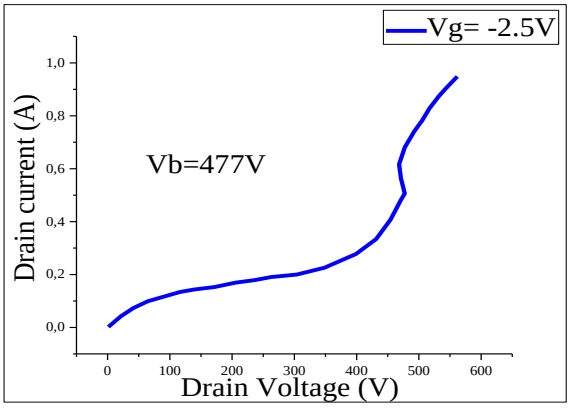

Figure 6. Off-state breakdown voltage simulation results.

The cause of the breakdown is defined as avalanche generation (impact ionization). The breakdown is due to the charge multiplication thatoccurs when the width of a space charge region is greater than the mean free path between twoionizing impacts. The reciprocal of the mean free path is called the ionization coefficient [36].

In this section, the gate voltage waskept at -2.5 V in order to have a very small drain current and simulate the off-state of the MOS-HEMT. The drain voltage was increased until the break criteria was reached. We can see from Figure.6 that for small values of the drain voltage, the increase in drain current is negligible.However, beyondaround 450V, even small variations of the drain voltage induce a large increase in the drain current. This is due to the breakdown of the device. Therefore, we can conclude that the breakdown voltage of the simulated model is close to 477V.

3.5. High-frequencyresults

The frequency performance of microwave devices can be evaluated through small-signal S-parameter simulations. from which several useful pieces of information can be extracted.

Cut off frequency f_T and maximum oscillation frequency f_{max} are two of them, representing important figures of merit as far as the frequency limits of the device is concerned. f_T is defined as the frequency at which forward current gain (H_{21}) from hybrid parameters becomes unity and f_{max} is defined as the frequency where the unilateral gain (U_g) or maximum stable gain (MSG) becomes unity [4]. The gains H_{21}, U_g and MSG were extracted directly from the simulated S-parameter data using the following equations.

$$H_{21} = \left|\frac{-2\,S_{21}}{(1-S_{11})\times(2-S_{22})-S_{12}\times S_{21}}\right| \quad (8)$$

$$U_g = \frac{|S_{21}|^2}{(1-|S_{11}|^2)\times(1-|S_{22}|^2)} \quad (5)$$

$$MSG = \frac{|S_{21}|}{|S_{12}|} \times (K \pm \sqrt{K^2-1}) \quad (6)$$

with

$$K = \frac{1-|S_{11}|^2-|S_{22}|^2+|S_{11}S_{22}-S_{12}S_{21}|^2}{2\times|S_{12}|^2\times|S_{22}|^2} \quad (7)$$

the stability factor.

Figure.7 shows the simulated S-parameters of the device at abias point V_{GS} = -2 V and V_{DS} = 15 V. The Simulation frequency range was from 0.1 GHz to 20.1 GHz, step-size of 0.1 GHz. Using the S-parameter simulation data and equations (4),(5), (6), and (7), the current gain H_{21}, the unilateral gain Ug and the Maximum Stable Gain (MSG) could be calculated as a function of frequency. Figure.8 shows the small signal characteristics of the proposed$TiO_2/Al_{0.3}GaN_{0.7}$/GaN MOS-HEMT device.

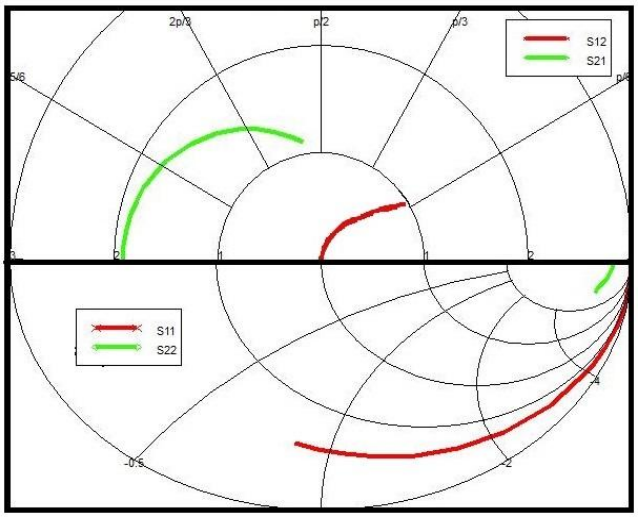

Figure 7. Typical simulated S-parameters of the MOS-HEMT.

The extraction process of f_T and f_{max} involves the S-parameters of the transistor ata selectedfrequency range (here from 0.1 GHz to 20.1 GHz) and a given bias point (V_{GS} = -2 V and V_{DS} = 15 V). Knowing that f_T is the frequency value where H_{21} becomes 0 dB and f_{max} where Ug or MSG becomes 0 dB [37], we found that f_T =229.83 GHz and f_{max}=627.58 GHz, an impressive value.

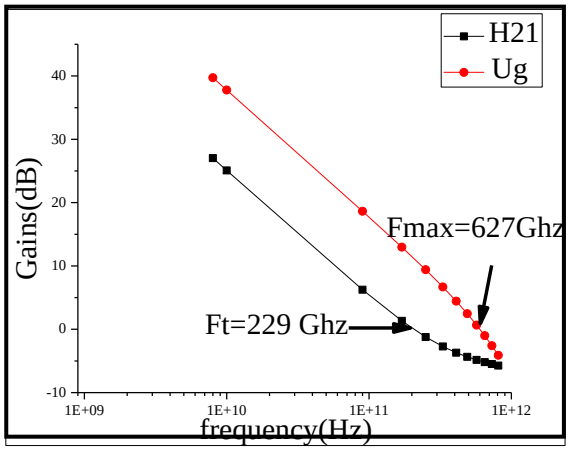

Figure 8. Small signal characteristics of the$TiO_2/AlGaN/GaN$ MOS-HEMT at the bias pointV_{GS} = -2 V and V_{DS} = 15 V.

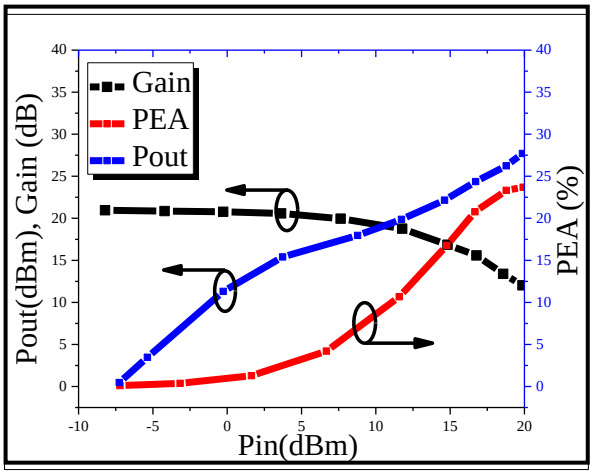

Figure 9. Power characteristics, (P_{out}, Gain and PAE) of theTiO_2/AlGaN/GaN MOS-HEMT at 10 GHz.

To characterize the power performance of the TiO_2/AlGaN/GaN MOS-HEMT at 10 GHz, ten large signal input amplitudes weredefined using WAVEFORMS statements. Each of these WAVEFORMS wereapplied to the gate in order to increasethe amplitude by using the LOOP statements [29]. Figure.9 shows the simulated typical output power and Power Added Efficiency (PAE) of the device. Table.3 reportsthe power characteristics of the simulated TiO_2/$Al_{0.3}GaN_{0.7}$/GaN MOS-HEMT atvarious bias conditions. The biasing operationsat V_{GS}= -2 V and -3 V can be classified as class A and AB, respectively.At abias of V_{GS}= -3V andV_{DS} = 10 V (class AB), a linear gain of 11.9 dB, a maximum output power of 20.26 dBm (531.44 mW/mm) and a maximum PAE of 26.43 %, were obtained. Athigher V_{GS}(V_{GS}= -2V) and with V_{DS} = 10V (class A), a higher linear gain of 13.11 dB, a higher maximum output power of 22.3 dBm (849.73 mW/mm) and a lower maximum PAE of 23.77 % were achieved. At V_{GS} = -3V, the maximum output power increased from 531 mW/mm to 754 mW/mm with increased V_{DS} (from 10V to 15V), which is the same as for V_{GS} = -2V. These results show the potential for TiO_2/$Al_{0.3}GaN_{0.7}$/GaNMOS-HEMT to produce millimeter wavelength power.

Table 3: Power characteristics under various bias conditions.

V_{GS}	V_{DS}	P_{out} Density (mW/mm)	Max PEA (%)	Linear gain (dB)
-2V	10V	577	23.6	12.7
-2V	15V	850	23.8	13.1
-3V	10V	531	26.5	11.9
-3V	15V	754	26.4	12.2

Table.4 demonstrates the performance of the proposed device by successful comparison of its effective channel thickness, peak f_T/f_{max}, and breakdown voltage with recent reported GaN MOS-HEMTs and HEMTs. In fact, by using the Regrown Source/Drain, the device exhibits a better I_{DS} atV_{GS} =4 V, an enhanced g_m, as well ashigher f_T / f_{max} and breakdown voltage while compared to other MOS-HEMTs devices.

Table 4: Performance Comparison with other dielectric MOS-HEMTs

	This work	Ref[38]	Ref[23]	Ref[16]	Ref[39]	Ref[25]	Ref[40]	Ref[41]	Ref[13]	Ref[42]
Oxide type	TiO_2	----	Al_2O_3	SiO_2	TiO_2	TiO_2	Al_2O_3	HfO_2	La_2O_3	TiO_2
Gate length(nm)	60	40	210	100	2000	1000	1000	100	1000	50
Regrown Source/Drain	Yes	Yes	Yes	Yes	No	No	---	No	No	No
f_T (GHz)	229	220	39.6	115	--	--	16.2	67	6.3	10.44
f_{max}(GHz)	627	289	39.8	127	--	--	18.4	94	10.7	13.8
breakdown voltage(V)	477	42	114	--	490	139	126	--	131	132
I_{DSS} (mA)	632	1620	860	950	380	384	552	580	572	550
g_m (mS/mm)	200	723	509	216	130	107	136	468	59.4	102
PAE (%)	26.43	--	--	--	--	--	16.4	--	--	--
sim/expr[1]	sim	expr	expr	expr	sim	expr	expr	sim	expr	expr

[1] sim/expr: simulation/experimental

4. Conclusion

The objective of this paper was to design and simulate a new MOS-HEMT model of an AlGaN/GaN HEMT with 60 nm gate-length, high-k TiO_2 gate dielectric and Regrown Source/Drain. The obtained simulated results are very encouraging whilecompared to existingAlGaN/GaN MOS-HEMTs (Table 4). This is,in fact, the best TiO_2/AlGaN/GaN MOS-HEMT simulated high-frequency performance reported so far, and thus, suitable for high-power RF circuit applications.

References

[1] K. Jena, R. Swain, and T. Lenka.Pramana.85.(2015) 1221.

[2] S.-i. Takagi and A. Toriumi.IEEE Trans. Electron Devices.42.(1995) 2125.

[3] F. M. Yigletu, S. Khandelwal, T. A. Fjeldly, and B. Iñiguez.IEEE Trans. Electron Devices.60.(2013) 3746.

[4] Z. e. Touati, Z. Hamaizia, and Z. Messai. *2015 4th International Conference on Electrical Engineering (ICEE)*.13-15 Dec. 2015.1.

[5] H. Pardeshi.SUPERLATTICE MICROST.88.(2015) 508.

[6] R. Swain, K. Jena, and T. Lenka.Mater Sci Semicond Process.53.(2016) 66.

[7] Z. Dong, J. Wang, C. P. Wen, D. Gong, Y. Li, M. Yu, Y. Hao, F. Xu, B. Shen, and Y. Wang.Solid State Electron.54.(2010) 1339.

[8] C.-C. Hu, M.-S. Lin, T.-Y. Wu, F. Adriyanto, P.-W. Sze, C.-L. Wu, and Y.-H. Wang.IEEE Trans. Electron Devices.59.(2012) 121.

[9] K.-T. Lee, C.-F. Huang, J. Gong, and C.-T. Lee.IEEE Electron Device Lett.32.(2011) 306.

[10] C.-S. Lee, Y.-H. Liao, B.-Y. Chou, H.-Y. Liu, and W.-C. Hsu.SUPERLATTICE MICROST.72.(2014) 194.

[11] Y. Liu, J. Li, W. Li, Q. Liu, Y. Yang, Y. Li, and Q. Chen.Int. J. Hydrog. Energy.40.(2015) 8856.

[12] H.-C. Chiu, C.-W. Yang, Y.-H. Lin, R.-M. Lin, L.-B. Chang, and K.-Y. Horng.IEEE Transactions on Electron Devices.55.(2008) 3305.

[13] C.-W. Lin, C.-W. Yang, C.-H. Chen, C.-K. Lin, and H.-C. Chiu. *Solid State Device Research Conference, 2009. ESSDERC'09. Proceedings of the European*. IEEE.435.

[14] C.-H. Hsu, W.-C. Shih, Y.-C. Lin, H.-T. Hsu, H.-H. Hsu, Y.-X. Huang, T.-W. Lin, C.-H. Wu, W.-H. Wu, and J.-S. Maa,Jpn. J. Appl. Phys.55.(2016) 04EG04.

[15] D. Meng, S. Lin, C. P. Wen, M. Wang, J. Wang, Y. Hao, Y. Zhang, K. M. Lau, and W. Wu.IEEE Electron Device Lett.34.(2013) 738.

[16] G. Hong-Yu, L. Yuan-Jie, G. Guo-Dong, D. Shao-Bo, F. Yu-Long, Z. Zhi-Rong, T. Xin, S. Xu-Bo, Z. Xing-Ye, and F. Zhi-Hong.Chin. Phys. Lett.32.(2015) 118501.

[17] D. Deen, D. Storm, D. Meyer, D. S. Katzer, R. Bass, S. Binari, and T. Gougousi.Phys. Status Solidi.8.(2011) 2420.

[18] S. Yang, S. Huang, M. Schnee, Q.-T. Zhao, J. Schubert, and K. J. Chen.IEEE Trans. Electron Devices.60.(2013) 3040.

[19] T. Hashizume, K. Nishiguchi, S. Kaneki, J. Kuzmik, and Z. Yatabe.Mater Sci Semicond Process.2017).

[20] Y. Hayashi, S. Kishimoto, and T. Mizutani.Solid State Electron.54.(2010) 1451.

[21] R. Stoklas, D. Gregušová, K. Hušeková, J. Marek, and P. Kordoš.Semicond. Sci. Technol.29.(2014) 045003.

[22] S. Dasgupta, D. F. Brown, F. Wu, S. Keller, J. S. Speck, and U. K. Mishra.Applied Physics Letters.96.(2010) 143504.

[23] T. Huang, Z. J. Liu, X. Zhu, J. Ma, X. Lu, and K. M. Lau.IEEE Trans. Electron Devices.60.(2013) 3019.

[24] S. A. Campbell, H.-S. Kim, D. C. Gilmer, B. He, T. Ma, and W. L. Gladfelter.IBM J Res Dev.43.(1999) 383.

[25] B.-Y. Chou, C.-S. Lee, C.-L. Yang, W.-C. Hsu, H.-Y. Liu, M.-H. Chiang, W.-C. Sun, S.-Y. Wei, and S.-M. Yu.IEEE Electron Device Lett.35.(2014) 1091.

[26] C.-S. Lee, W.-C. Hsu, B.-Y. Chou, H.-Y. Liu, C.-L. Yang, W.-C. Sun, S.-Y. Wei, S.-M. Yu, and C.-L. Wu.IEEE Trans. Electron Devices.62.(2015) 1460.

[27] H. Liu, C. Lee, W. Hsu, T. Wu, H. Huang, S. Chen, Y. Yang, B. Chiang, and H. Chang. *2015 IEEE 11th International Conference on Power Electronics and Drive Systems*. IEEE.578.

[28] T. L. SEOW, "STUDY OF TRAPPING EFFECTS IN ALGAN/GAN MOSHEMTS," 2015.

[29] SILVACO, " vol. 1, ed, 2014.

[30] O. Breitschädel, L. Kley, H. Gräbeldinger, J. Hsieh, B. Kuhn, F. Scholz, and H. Schweizer.Materials Science and Engineering: B.82.(2001) 238.

[31] Z. Li and T. P. Chow.Solid State Electron.56.(2011) 111.

[32] P. S. Park and S. Rajan.IEEE Trans. Electron Devices.58.(2011) 704.

[33] J. M. Tirado, J. L. Sanchez-Rojas, and J. I. Izpura.IEEE Trans. Electron Devices.54.(2007) 410.

[34] X. Zheng, S. Feng, Y. Zhang, and J. Yang.Microelectron Reliab.63.(2016) 46.
[35] P. Nakkala, "Pulsed IV and RF characterization and modeling of AIGaN HEMTs and Graphene FETs," Université de Limoges, 2015.
[36] S. Yagi, M. Shimizu, M. Inada, Y. Yamamoto, G. Piao, H. Okumura, Y. Yano, N. Akutsu, and H. Ohashi.Solid State Electron.50.(2006) 1057.
[37] Z. Kourdi, B. Bouazza, A. Guen-Bouazza, and M. Khaouani.Microelectron Eng.142.(2015) 52.
[38] K. Shinohara, A. Corrion, D. Regan, I. Milosavljevic, D. Brown, S. Burnham, P. Willadsen, C. Butler, A. Schmitz, and D. Wheeler. *Electron Devices Meeting (IEDM), 2010 IEEE International*. IEEE.30.1. 1.
[39] X. Li, J. Wang, J. Cai, Y. Liu, Z. Yang, B. Zhang, M. Wang, M. Yu, B. Xie, and W. Wu.ECS Transactions.52.(2013) 841.
[40] H.-Y. Liu, B.-Y. Chou, W.-C. Hsu, C.-S. Lee, J.-K. Sheu, and C.-S. Ho.IEEE Trans. Electron Devices.60.(2013) 213.
[41] S. K. Swain, S. Adak, S. K. Pati, and C. K. Sarkar.SUPERLATTICE MICROST.97.(2016) 258.
[42] Y. S. Lin, C. C. Lu, and W. C. Hsu.Phys. Status Solidi.14.(2017).